Available online at www.sciencedirect.com
SCIENCE DIRECT
Journal of Constructional Steel Research 62 (2006) 793–801
JOURNAL OF CONSTRUCTIONAL STEEL RESEARCH
www.elsevier.com/locate/jcsr

Ductile moment connections used in steel column-tree moment-resisting frames

Cheng-Chih Chen*, Chun-Chou Lin, Chieh-Hsiang Lin

[a] *Department of Civil Engineering, National Chiao Tung University, 1001 Ta Hsueh Road, 30010 Hsinchu, Taiwan*

Received 17 May 2005; accepted 30 November 2005

Abstract

This paper presents analytical and experimental studies on the cyclic behavior of beam-to-column moment connections used in steel column-tree moment-resisting frames. The column-tree system is joining the column-trees and link beams in the field while the column-trees are fabricated in the shop by welding stub beams to the column. The proposed ductile column-tree connections have two distinctively improved connection details which are no weld access hole detail and a widened flange of the stub beam. Nonlinear finite element analysis demonstrated the effectiveness of the improved connection details which significantly reduce the stress concentration and plastic strain demands at the beam flange groove weld. Cyclic testing of three full-scale specimens was conducted to verify the proposed connection details. All the specimens successfully developed ductile behavior with no brittle fracture by forming the plastic hinging of the beam away from the beam–column interface. The widened flange and no weld access hole details are effective in reducing the potential of brittle fracture.

Keywords: Column-tree; Moment connection; Plastic strain; Weld access hole

1. Introduction

Moment-resisting frames are frequently used in regions of high seismic risk to resist seismic force. The moment connections of the moment-resisting frame are designed to connect the beam flange to the column using a complete joint penetration (CJP) groove weld in the field. A typical beam-to-column connection detail of a moment connection prior to the 1994 Northridge earthquake is shown in Fig. 1. Many connections, however, failed in a brittle manner during the Northridge earthquake. Brittle fractures occurred at the beam-to-column joint, resulting from several factors such as stress concentration in weld access hole regions, initiating crack due to back-up bars at the beam bottom flanges, weld defects, and material deficiencies [1,2]. To prevent the premature failure of the joint, various improved details have been proposed in the aftermath of the Northridge earthquake. Post-Northridge connections include reduced beam section connections [3–5] and reinforced connections [6–8] that enable the required performance to be developed under cyclic loading.

A column-tree system is one of the constructional schemes used for the moment-resisting frame. The column-tree is fabricated by welding stub beams to the column in the shop. Unlike the pre-Northridge connection case, the critical welding of the beam-to-column joint is performed in the shop, which can provide a better quality control. The stub beam is generally 600 to 1000 mm long. A mid-portion of the beam is then spliced to the stub beam to form the moment-resisting frame after the shop fabricated column-trees are erected in the field. Fig. 2 illustrates the column-tree construction. There are various options for the splice joining the link beam to the column-tree [9]. Fig. 3 shows two beam splice options frequently used: one is field-bolted connection; the other is web-bolted flange-welded connection. The use of the field-bolted splice connection can speed the erection and reduce the field erection costs. Nevertheless, the use of the field-welded splice connection can eliminate possible slippage of the bolted splice connection during major earthquakes. On the other hand, the splice connection can be designed to provide stable hysteretic behavior by reducing the flange splice plate section as proposed by McMullin and Astaneh-Asl [10]. Of

* Corresponding author. Tel.: +886 3 571 2121x54915; fax: +886 3 572 7109.
E-mail address: chrischen@mail.nctu.edu.tw (C.-C. Chen).

0143-974X/$ - see front matter © 2005 Elsevier Ltd. All rights reserved.
doi:10.1016/j.jcsr.2005.11.012

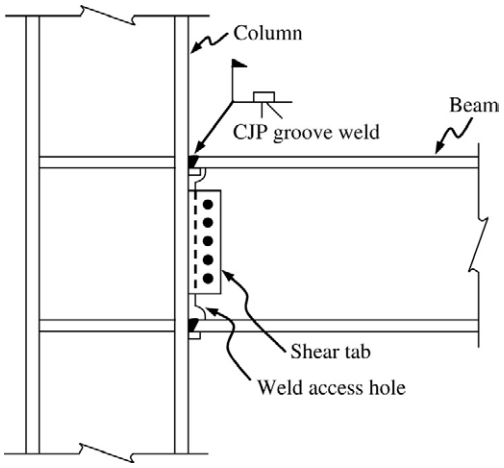

Fig. 1. Typical pre-Northridge moment connection.

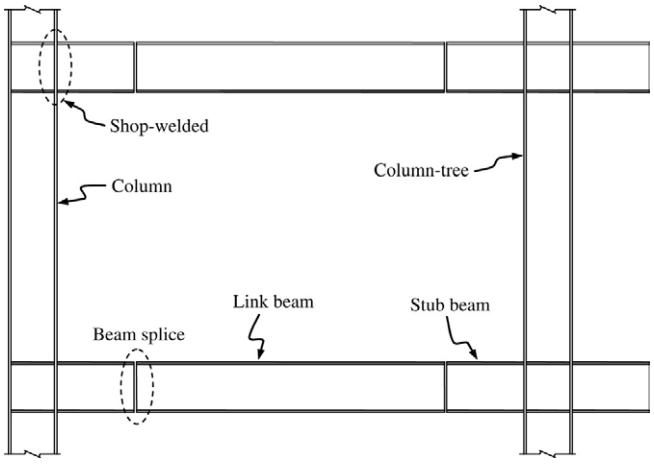

Fig. 2. Column-tree construction.

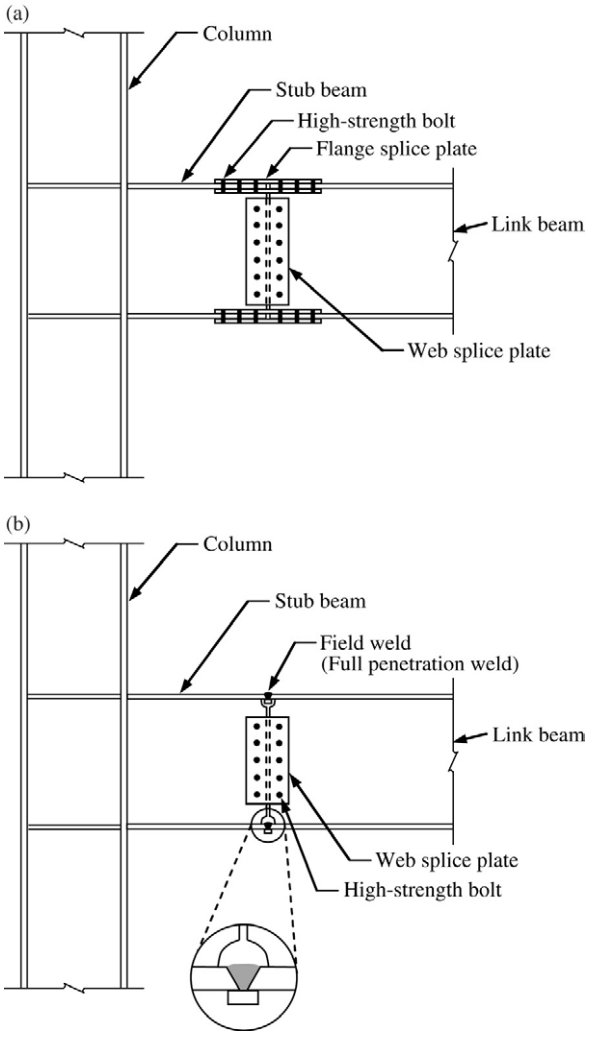

Fig. 3. Beam splice options joining the link beam to the column-tree.

course, it is inevitable that the column-trees cost more for transportation and handling; however, the use of the column-tree frame can reduce the cost in the field.

The column-tree construction has been widely used in Japan, and the column-tree systems are frequently in the shop-welded, field-bolted form. However, a number of column-tree connections were damaged during the 1995 Kobe earthquake [11]. Brittle fracture was observed in the shop welding connections although the shop-welded connection was believed to have better quality than field-welded connection. To achieve the desired performance of the column-tree construction, this study analytically and experimentally investigates the cyclic behavior of the column-tree connection by improving the connection details. Nonlinear finite element analysis was performed to study the effects of the design parameters on the inelastic behavior. A full-scale experiment was further conducted to clarify the cyclic performance of the proposed connection details for column-tree construction.

2. Widened flange column-tree connection

As indicated in Fig. 1, weld access holes (WAH) in the beam web are necessary for performing the CJP groove weld

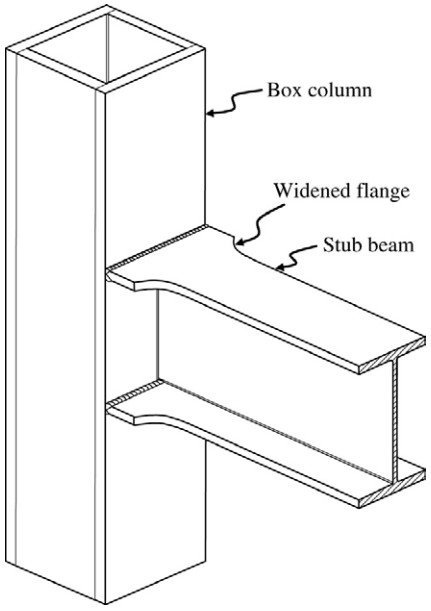

Fig. 4. Widened flange connection for the column-tree.

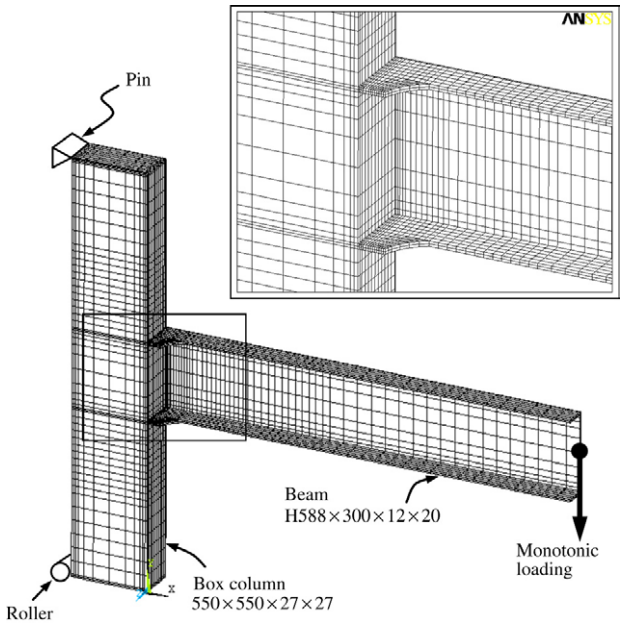

Fig. 5. Three-dimensional finite element modeling.

Table 1
Properties of subassemblages

Finite element model	Specimen designation	Max. width of widened flange (mm)	Length of widened flange (mm)	Length of stub beam (mm)
W10-L1A	W10-L1	550	200	1000
W10-L2A	W10-L2	550	400	1000
W08-L1A	W08-L1	440	200	1000
UW	–	(unwidened)	–	–

joining the beam flange to the column flange. The presence of the WAHs, however, creates concentrations of the stresses and highest fracture potential in the joint that has been addressed in the literature [12,13]. The localized stress concentration initiates cracking in the WAH regions and consequently leads to fracture of the beam flange, as observed in the beam-to-column connections after the earthquake [2,11] or in the laboratory [13,14]. Having the advantage of fabrication in the shop, the proposed column-tree connection was designed without WAH to prevent the possible fracturing of the beam flange caused by the WAH.

The improved scheme of the post-Northridge connections, with either the reduced beam section connections or the reinforced connections, is forcing the plastic hinging of the beam away from the column face. The reduced beam section connection fulfills this requirement by trimming the beam flange, whereas the reinforced connection does it by strengthening the beam section near the column. A widened flange connection is proposed in this study, obtained by enlarging the beam flange in the beam-to-column joint. Fig. 4 shows the configuration of the proposed column-tree connection. The beam stub is built up using the widened flange and the web plates. The widened beam flange is intended to reinforce the beam-to-column joint and form the plastic hinge away from the column face. Rather than stiffening being

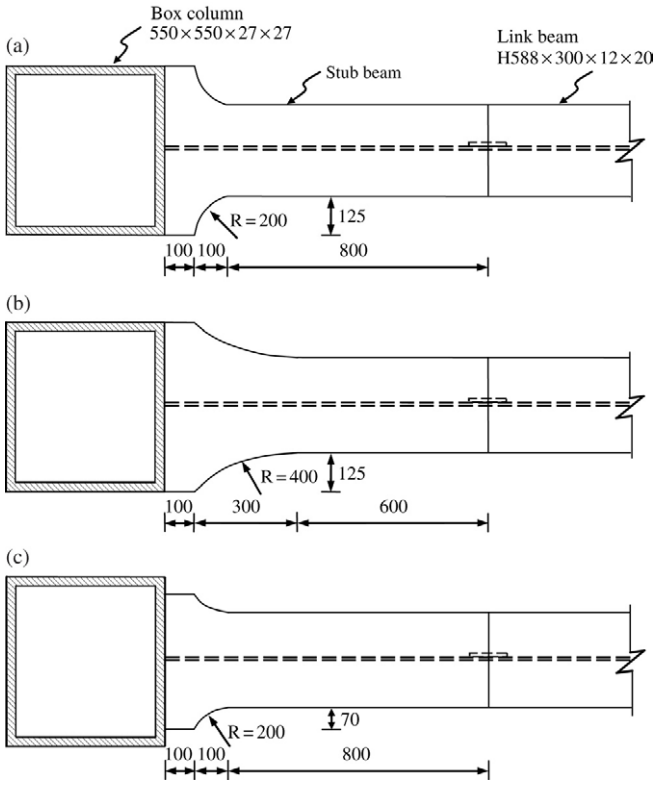

Fig. 6. Column-tree moment connection models: (a) W10-L1A; (b) W10-L2A; (c) W08-L1A.

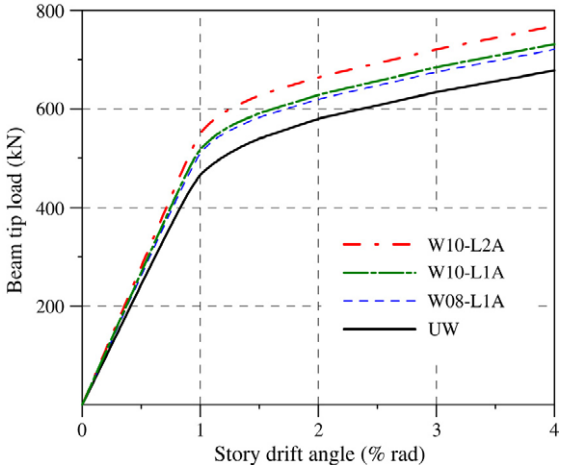

Fig. 7. Beam tip load versus story drift angle relations for analytical models.

provided by a flat triangular stiffener on both sides of the beam flange, a piece of the beam flange plate with a curved transition is used to provide smooth force transference. Nonlinear finite element analyses and experiments were carried out to clarify the seismic performance of the widened flange connection.

3. Numerical investigation

3.1. Finite element modeling

Using nonlinear finite element analysis, the analytical study was conducted for various configurations of the widened

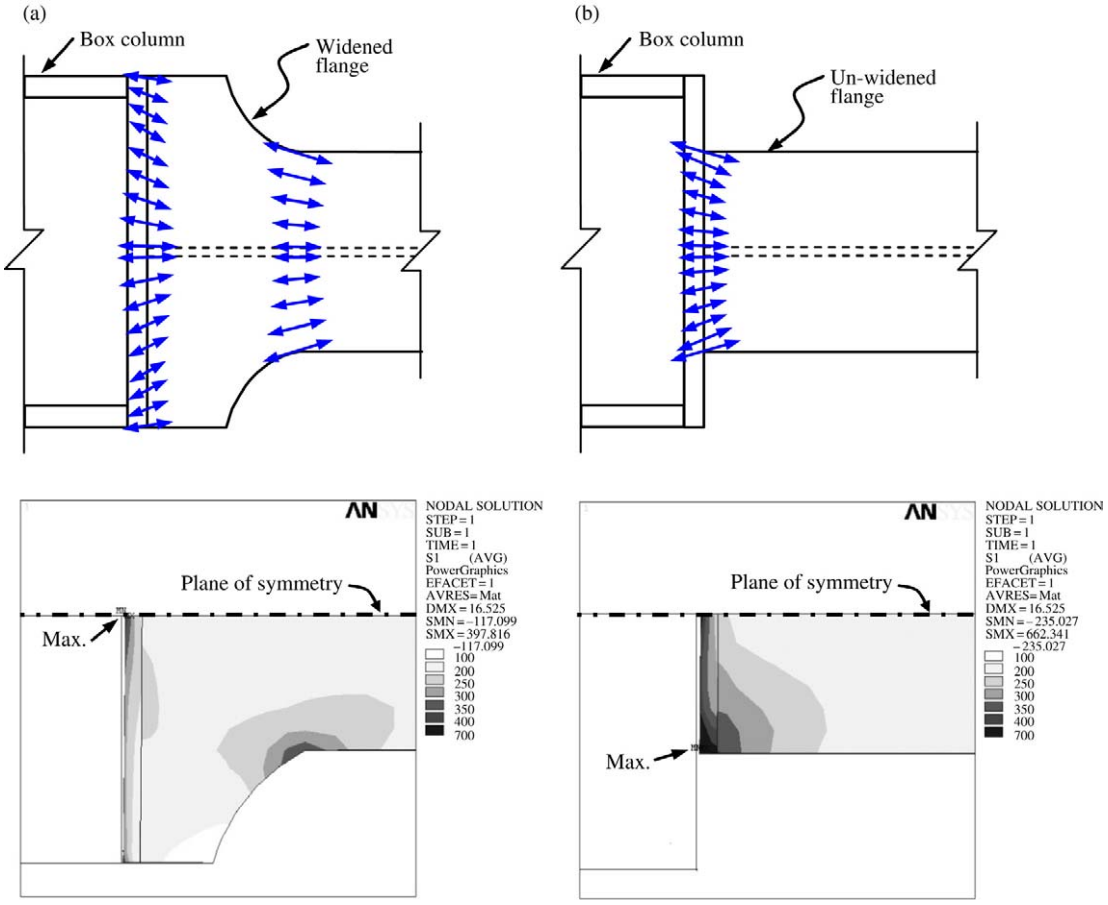

Fig. 8. Distributions of principal stress vectors and contours at the beam–column interface at 0.5% rad story drift angle: (a) W10-L1A; (b) UW.

flange connection. A previously validated modeling using a general purpose nonlinear finite element program [15] was employed to model the subassemblage of the connection [13]. The subassemblage represents an exterior beam-to-column connection, isolated from a moment frame at the inflection points of the column and the beam. The subassemblage consists of an H-shaped H588 × 300 × 12 × 20 (dimensions in mm for depth, width, web thickness, and flange thickness, respectively) beam, 3030 mm long and a box column of 550 × 550 × 27 × 27 with 3000 mm span length. Fig. 5 shows the three-dimensional finite element modeling. Linear elastic and strain hardening behavior was assumed for ASTM A572 Grade 50 steel used for the column and the beam. More details related to the element and material modeling can be found in the literature [13].

The box column has a great capacity to resist biaxial bending. Therefore, box columns are commonly used in some high seismic risk regions such as Taiwan and Japan. However, as revealed by previous studies, at the beam–column interface, high stress concentration occurs at both tips of the beam flanges, which initiates cracking from the beam flange tips [16]. The widened flange is proposed for use for box columns to eliminate this inherent deficiency.

On the basis of the concept of the widened flange connection, two major design parameters were studied: the maximum width and the length of the enlarged beam flange. Four different configurations of the connections were modeled as presented in Table 1. The connection with the unwidened flange was designated as “UW”, which represents an unreinforced connection. To clarify the effect of the maximum width of the enlarged beam flange on the connection behavior, two maximum widths were adopted. The ratios of the maximum widened flange width to the column width are set to 1.0 (for W10-L1A and W10-L2A) and 0.8 (for W08-L1A). To ensure plastic hinge formation away from the column face, the length of the enlarged beam flange was designed as either 200 mm or 400 mm, which are represented in the labeling of the connection with L1 and L2, respectively. Fig. 6 shows the details for these three widened flange connections.

3.2. Discussion of the analysis results

Beam tip load versus story drift angle curves for all the numerical models are shown in Fig. 7. The story drift angle is computed as the ratio of the beam tip displacement to the distance between the beam tip and the column centerline. All models demonstrated elastic behavior before 1% rad story drift angle which is usual for typical moment frames. Due to the reinforcement of the widened flange, the models with a widened flange displayed slightly higher elastic stiffness and inelastic strength than the unwidened flange model UW.

A story drift angle of 0.5% rad was chosen to elucidate the response of the subassemblages in the elastic range because

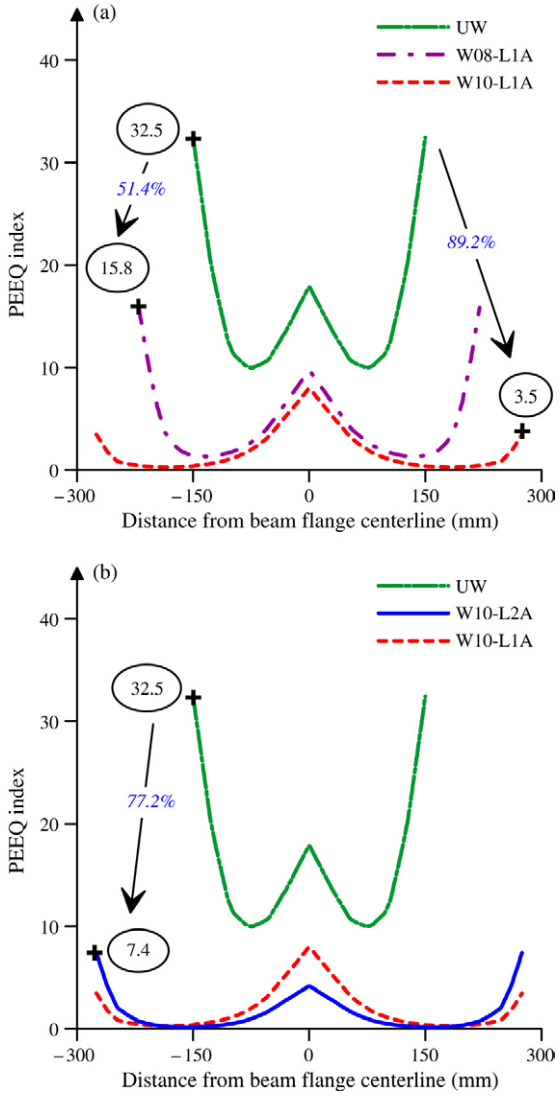

Fig. 9. Distributions of PEEQ indices along the beam flange groove weld at 4% rad story drift angle: (a) effects of widened flange width; (b) effects of widened flange length.

numerous moment connections damaged in premature fracture with very limiting plastic behavior during the earthquake. To evaluate the potential brittle fracture, the principal stress is presented for comparison because the cracking generally developed at the location of greatest principal stress. Fig. 8 shows the principal stress vectors and stress contours of models W10-L1A and UW, at 0.5% rad story drift angle, at the beam flange groove weld which is the most critical location for the moment connection. The size of the stress vector also indicates the magnitude of the stress. The largest value of the principal stress normalized by the yield strength of the beam material was up to 1.9 for UW, whereas its value was merely 1.14 for W10-L1A. The stress in UW was maximum at the edges of the beam flange, while the maximum stress in W10-L1A occurred at the centerline of the beam flange.

The connection behavior in the inelastic range can be examined through the plastic strain. To evaluate the local plastic strain demand, the response of the subassemblages is presented in terms of the PEEQ index which has been used by other researchers [12,17]. The abbreviation PEEQ stands for “plastic equivalent strain”, which represents the local plastic strain demand. The PEEQ index is defined as the ratio of PEEQ to the yield strain. Certainly, a higher PEEQ index indicates a higher demand for plastic strain. A story drift angle of 4% rad was used to compare the connection behaviors under highly strained states because a special moment-resisting frame is assumed to be capable of sustaining a story drift angle of at least 4% rad [18].

Fig. 9 plots the distributions of the PEEQ indices along the beam flange groove weld at 4% rad story drift angle. For model UW, peak PEEQ indices were observed at the extreme edges of the beam flange groove weld. When the widened flange was used, the maximum PEEQ index decreased by 51.4% for W08-L1A (reduced from 32.5 to 15.8) and 89.2% for W10-L1A (reduced from 32.5 to 3.5), compared to that of UW. It is clear that a wider flange at the beam–column interface results in a lower PEEQ index. The narrower widened flange of W08-L1A represents a more critical condition because the stress and strain demands along the beam flange groove weld were increased. Fig. 9(b) shows the distributions of the PEEQ indices for subassemblages with different lengths of the widened flange. Increasing the length of the widened flange from 200 mm (W10-L1A) to 400 mm (W10-L2A) has an insignificant effect on the local plastic strain demand.

To elucidate the plastification and plastic hinge formation for the widened flange connection, the distributions of the plastic equivalent strain at various loading steps are shown, to demonstrate the spread of the yielding zone. Fig. 10 displays the progressive contours of the plastic equivalent strain at 1, 1.5 and 4% rad story drift angles. The highest plastic equivalent strain did not occur in the beam flange groove weld. Notably, extensive yielding took place in the beam flange beyond the widened flange. On the basis of the spread of the yielding zone shown in the figures, indeed, the plastic hinge formed away from the beam–column interface. In brief, the distributions of the plastic equivalent strain exhibit that the widened flange connection can develop extensive inelastic behavior in the beam section away from the column face.

4. Experimental investigation

4.1. Test specimens

An experiment was carried out to clarify the cyclic behavior of the column-tree connections with a widened flange. Three full-scale specimens were designed to represent an exterior beam-to-column subassemblage under the seismic loading condition. The specimens had the same size and geometry as the subassemblages used in the finite element analysis. The specimen designation is presented in Table 1.

Both the beam and column are all ASTM A572 Grade 50 steel. The shape of the widened flange was fabricated by a flame cutting process and was then ground with a hand grinder. Fig. 11 depicts the welding details for the specimens without the weld access hole detail. The short stub of the beam was

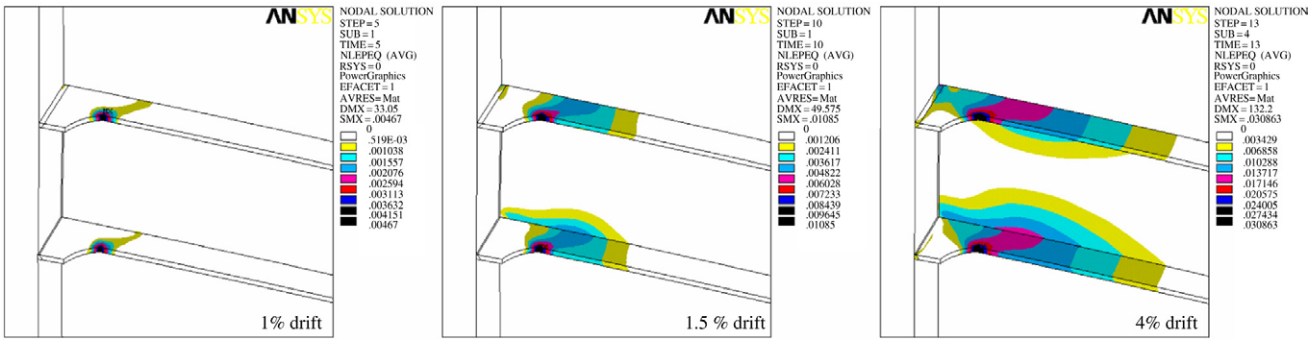

Fig. 10. Plastic equivalent strain contours of W10-L1A at 1, 1.5 and 4% rad story drift angles.

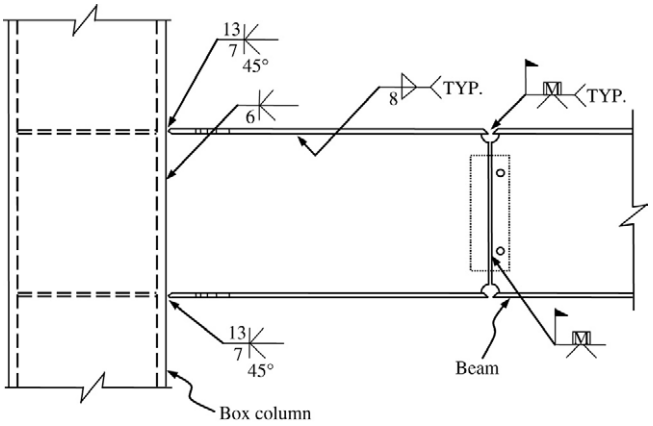

Fig. 11. Welding details for specimens.

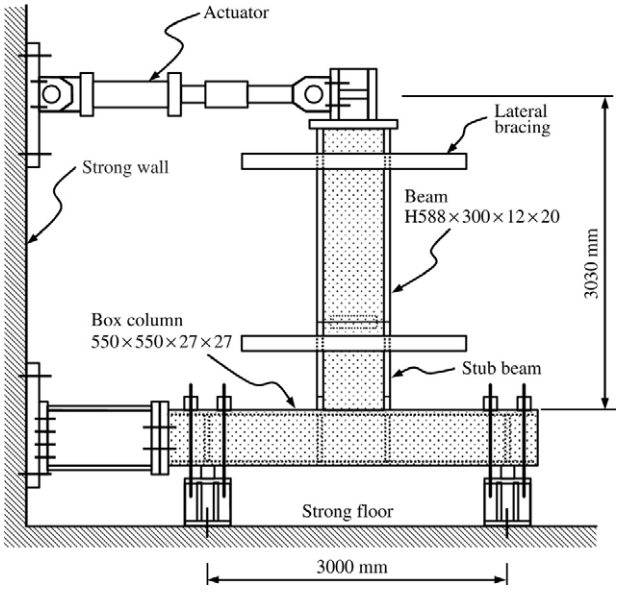

Fig. 12. Schematic diagram of the test set-up.

built up to form the widened flange stub beam. The beam flanges were double bevel groove welded to the column flange. A large size of the bevel groove weld was used inside the beam flange to allow the defective weldment to be easily gouged from outside the beam flange. The remaining bevel groove weld was consequently completed from outside the beam flange. Although the splice of the link beam to the column-tree in

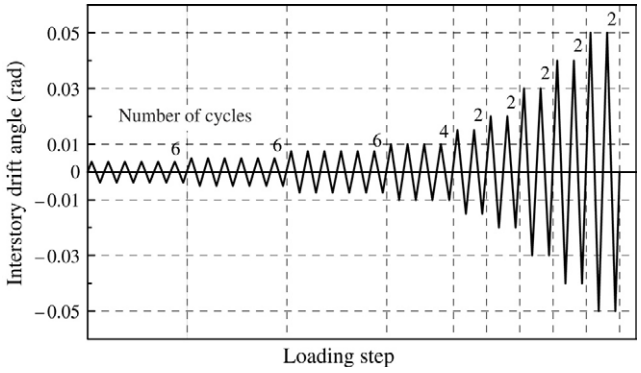

Fig. 13. Loading sequence.

practice can be field bolted, herein the splice was fully welded to prevent any influence of splice slippage on the behavior of the widened flange connection. The extra cost for the widened flange is comparatively minor, compared to that of the overall column-tree construction.

4.2. Test set-up and procedure

The schematic diagram of the test set-up is shown in Fig. 12, which simulates the boundary conditions of the subassemblage. As shown in Fig. 13, the loading sequence specified in the AISC seismic provisions [18] was followed for the cyclic testing. The sequence began with six successive cycles at the story drift angles of 0.375%, 0.5% and 0.75% rad. Afterward, four cycles of 1% rad and two cycles of over 1.5% rad were followed until failure occurred. To conduct the cyclic testing, a predetermined cyclic displacement history was applied at the beam tip by a hydraulic actuator.

4.3. Discussion of the test results

All three specimens behaved very similarly, although different details of the widened flange were used. As evidenced by the flaking of the whitewash, yielding of the specimens occurred initially at the edges of the curved part of the widened flange as observed in the finite element analysis. During the cycles of 3% rad story drift angle, a great amount of the whitewash conspicuously flaked and expanded into the beam flange and the nearby beam web. Local buckling of the beam flanges was noticed in the cycles with 4% rad story drift angle.

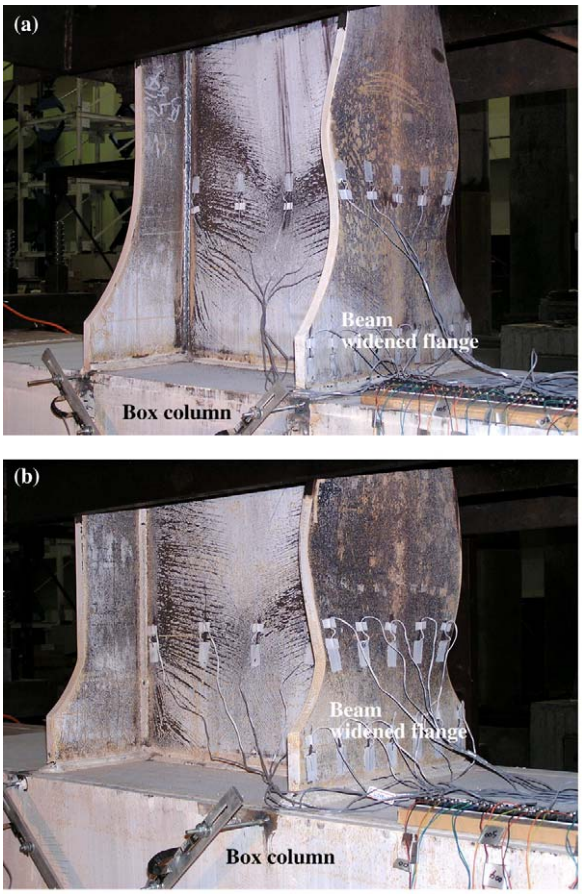

Fig. 14. Yielding and local buckling at 4% rad story drift angle: (a) W10-L2; (b) W08-L1.

Fig. 14 shows the yielding and local buckling of specimens W10-L2 and W08-L1. In the cycles of 5% rad story drift angle, excessive buckling of the beam section caused gradual deterioration in the strength. For all the specimens, the plastic hinging of the beam formed reliably in the beam section away from the column face, assuring sufficient inelastic deformation of the connection. At the end of the tests, no signs of fracturing were observed except that minor cracking was noticed at the edge of the widened flange of specimen W10-L1 during the second cycle of 5% rad story drift angle, as shown in Fig. 15.

Cyclic behavior of the subassemblage is generally evaluated through the hysteretic loops of load versus displacement as well as the hysteretic loops of normalized moment versus total plastic rotation. The test moment was calculated from the beam tip load multiplying the overall beam length. The test moment was further normalized by the plastic flexural strength of the beam section, using the material strengths measured from the coupon tests. It should be noted that the ratio of the test moment to the plastic flexural strength indicates the level of the beam section that has been stressed. The total plastic rotation for the subassemblage was determined by subtracting the elastic rotation from the story drift angle.

Fig. 16 presents the hysteretic loops of the beam tip load versus beam tip displacement as well as the hysteretic loops of the normalized moment versus total plastic rotation for all three specimens. Because the column and the panel zone

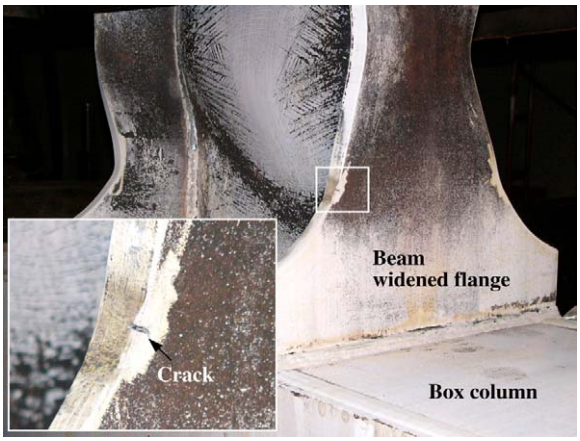

Fig. 15. Minor cracking on the widened flange of specimen W10-L1 at 5% rad story drift angle.

behaved elastically throughout the testing, the plastic rotation of the subassemblage was contributed merely from the inelastic deformation of the beam. The formation of the plastic hinge in the beam section was the only source credited to the plastic rotation. As demonstrated in Fig. 16, the hysteretic loops show stable and reliable cyclic behavior. The gradual strength deterioration as observed in the hysteretic loops was caused by the local buckling of the beam flange and the web. All the specimens can develop reliable inelastic behavior with maximum story drift angles greater than 5% rad, which represent the maximum total plastic rotations ranging from 4% to 4.9% rad. Envelope curves of the beam tip load–displacement hysteretic curves are shown in Fig. 17. Identical global behavior was obtained for the specimens. In fact, the width and length of the widened flange have very little effect on the global behavior of the subassemblage.

Table 2 shows the maximum test moments and calculated plastic flexural strengths of the specimens at the locations of the column face and plastic hinge. The plastic hinge location is defined as at the far end of the curved part of the widened flange from the column face. The ratios of the maximum test moment to the calculated plastic flexural strength at the column face, $M_{j,\text{test}}/M_{pj}$, range from 0.77 to 0.98. These ratios indicate that the connection reserved flexural strength at the beam–column joint. However, the ratios $M_{j,\text{test}}/M_{pj}$ for specimen W08-L1 are 0.97 and 0.98 which imply that this widened flange barely provides the required flexural strength because of the use of the smaller width than for other specimens. Although the global behavior of specimen W08-L1 was almost identical to those of other specimens, the local strength demand at the column face is much higher for W08-L1 as can be seen from the greater ratios $M_{j,\text{test}}/M_{pj}$ than for other specimens. Moreover, the ratios of the maximum test moment to the calculated plastic flexural strength at the plastic hinge, $M_{ph,\text{test}}/M_p$, range from 1.17 to 1.24. Large inelastic deformation with strain-hardening behavior was expected at the plastic hinge location because these ratios are well beyond unity. Plastic hinging of the beam away from the column face is also evidenced from these comparisons.

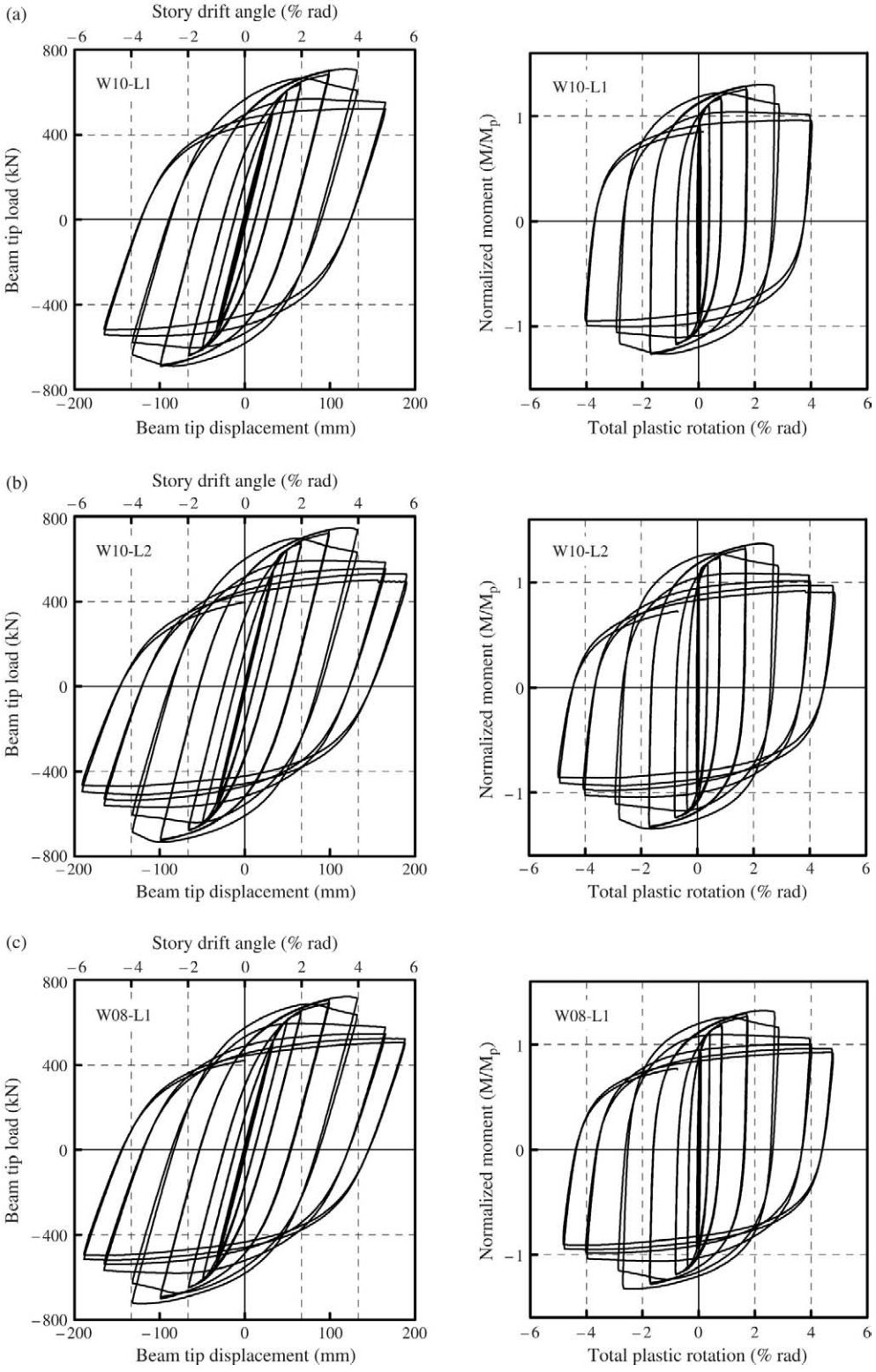

Fig. 16. Beam tip load versus beam tip displacement curves and normalized moment versus total plastic rotation curves for specimens: (a) W10-L1; (b) W10-L2; (c) W08-L1.

5. Conclusions

A preliminary investigation of the cyclic behavior of the widened flange connection proposed for the steel column-tree moment-resisting frames has been presented in this study. As revealed by the finite element analysis, the widened flange connection associated with no weld access hole detail can diminish the potential for brittle fracture caused by the peak plastic strain demand in the weld access hole region as existing in a pre-Northridge connection. Further, extensive

Table 2
Flexural strength summary

Specimen designation	Maximum test moment		Calculated plastic flexural strength		Ratio of test moment to calculated strength	
	At column face $M_{j,\text{test}}$ (kN m)	At plastic hinge $M_{ph,\text{test}}$ (kN m)	At column face M_{pj} (kN m)	At plastic hinge M_p (kN m)	At column face $\frac{M_{j,\text{test}}}{M_{pj}}$	At plastic hinge $\frac{M_{ph,\text{test}}}{M_p}$
W10-L1	+2147	+2005	2712	1652	0.79	1.21
	−2091	−1953			0.77	1.18
W10-L2	+2263	+1964	2712	1652	0.83	1.19
	−2223	−1929			0.82	1.17
W08-L1	+2188	+2043	2246	1652	0.97	1.24
	−2193	−2049			0.98	1.24

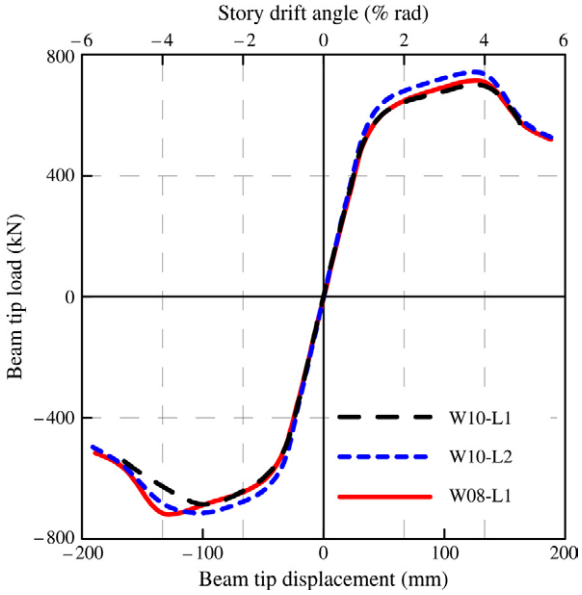

Fig. 17. Envelope curves of beam tip load–displacement relations.

yielding and plastification occurred in the curved part of the widened flange ensuring the formation of a plastic hinge. The cyclic performance of the widened flange connection has been confirmed by the tests conducted for three full-scale specimens. All the specimens showed ductile behavior by forming a plastic hinge in the beam section away from the column face owing to the intended effect of the widened flange. The proposed connection can achieve code requirements for inelastic deformation and flexural resistance for special moment frames. Further research, however, is needed to address the application of the improved connection details to different sizes of beams and columns or H-shaped column sections, because only a limited number of tests were conducted in this study.

Acknowledgment

The authors would like to thank the National Science Council of the Republic of China, Taiwan, for financially supporting this research.

References

[1] Mahin ST. Lessons from damage to steel buildings during the Northridge earthquake. Engineering Structures 1998;20(4–6):261–70.
[2] Miller DK. Lessons learned from the Northridge earthquake. Engineering Structures 1998;20(4–6):249–60.
[3] Chen SJ, Yeh CH, Chu JM. Ductile steel beam-to-column connections for seismic resistance. Journal of Structural Engineering 1996;122(11): 1292–9.
[4] Plumier A. The dogbone: back to the future. Engineering Journal, AISC 1997;(second quarter):61–7.
[5] Engelhardt MD, Winneberger T, Zekany AJ, Potyraj TJ. Experimental investigation dogbone moment connections. Engineering Journal, AISC 1998;(4th quarter):128–39.
[6] Uang CM, Bondad D, Lee CH. Cyclic performance of haunch repaired steel moment connections: experimental testing and analytical modeling. Engineering Structures 1998;20(4–6):552–61.
[7] Engelhardt MD, Sabol TA. Reinforcing of steel moment connections with cover plates: benefits and limitations. Engineering Structures 1998; 20(4–6):510–20.
[8] Lee CH. Seismic design of rib-reinforced steel moment connections based on equivalent strut model. Journal of Structural Engineering 2002;128(9): 1121–9.
[9] Astaneh-Asl A. Seismic design of steel column-tree moment-resisting frames. Steel tips, Structural Steel Educational Council. 1997. pp. 40.
[10] McMullin KM, Astaneh-Asl A. Steel semirigid column-tree moment resisting frame seismic behavior. Journal of Structural Engineering 2003; (9):1243–9.
[11] Nakashima M, Inoue K, Tada M. Classification of damage to steel buildings observed in the 1995 Hyogoken-Nanbu earthquake. Engineering Structures 1998;20(4–6):271–81.
[12] Lu LW, Ricles JM, Mao C, Fisher JW. Critical issues in achieving ductile behaviour of welded moment connections. Journal of Constructional Steel Research 2000;55(1–3):325–41.
[13] Chen CC, Chen SW, Chung MD, Lin MC. Cyclic behaviour of unreinforced and rib-reinforced moment connections. Journal of Constructional Steel Research 2005;61(1):1–21.
[14] Stojadinovic B, Goel SC, Lee KH, Margarian AG, Choi JH. Parametric tests on unreinforced steel moment connections. Journal of Structural Engineering 2000;126(1):40–9.
[15] ANSYS User Manual. ANSYS, Inc.; 2001.
[16] Roeder CW. General issues influencing connection performance. Journal of Structural Engineering 2002;128(4):420–8.
[17] El-Tawil S, Mikesell T, Kunnath SK. Effect of local details and yield ratio on behavior of FR steel connections. Journal of Structural Engineering 2000;126(1):79–87.
[18] AISC. Seismic provisions for structural steel buildings. Chicago (IL) American Institute of Steel Construction; 2002.